



Research articles

Effect of Nb on magnetic and mechanical properties of TbDyFe alloys

Naijuan Wang^a, Yuan Liu^{a,b,*}, Huawei Zhang^{a,b}, Xiang Chen^{a,b}, Yanxiang Li^{a,b}^a School of Materials Science and Engineering, Tsinghua University, Beijing 100084, PR China^b Key Laboratory for Advanced Materials Processing Technology, Ministry of Education, PR China

ARTICLE INFO

Article history:

Received 25 July 2017

Accepted 12 October 2017

Available online 16 October 2017

Keywords:

TbDyFe alloy

Microstructure

Magnetostriptive properties

Mechanical performance

ABSTRACT

The intrinsic brittleness in giant magnetostriptive material TbDyFe alloy has devastating influence on the machinability and properties of the alloy, thus affecting its applications. The purpose of this paper is to study the mechanical properties of the TbDyFe alloy by alloying with Nb element. The samples $(\text{Tb}_{0.3}\text{Dy}_{0.7})_x\text{Fe}_{2x}\text{Nb}_y$ ($y = 0, 0.01, 0.04, 0.07, 0.1$; $3x + y = 1$) were melted in an arc melting furnace under high purity argon atmosphere. The microstructure, magnetostriptive properties and mechanical performance of the alloys were studied systematically. The results showed that NbFe_2 phases were observed in the alloys with the addition of Nb. Moreover, both the NbFe_2 phases and rare earth (RE)-rich phases were increased with the increasing of Nb element. The mechanical properties results revealed that the fracture toughness of the alloy with the addition of Nb enhanced 1.5–5 times of the Nb-free alloy. Both the NbFe_2 phase and the RE-rich phase had the ability to prevent crack propagation, so that they can strengthen the REFe_2 body. However, NbFe_2 phase is a paramagnetic phase, which can reduce the magnetostriptive properties of the alloy by excessive precipitation.

© 2017 Elsevier B.V. All rights reserved.

1. Introduction

The magnetostriptive effect was first discovered in the 19th century (1842) by an English physicist James Joule [1]. He observed that a sample of ferromagnetic material, i.e. iron, changes its length in the presence of applied magnetic field. Comparisons of performances from different magnetostriptive materials are most often made on the basis of the magnetostriptive strains they can generate. One of the best new magnetostriptive materials known as Terfenol-D, typically $\text{Tb}_{0.3}\text{Dy}_{0.7}\text{Fe}_{1.95}$, processes a good trade-off between high room magnetostriptive strains and low magnetostriiction crystal anisotropy constant [2,3]. Currently, a wide variety of applications in micro-positioners, fluid injectors, active damping systems, helicopter blade control systems, as well as some hybrid-applications have been introduced into the public domain [4–7].

Many researches aimed to improve the magnetic properties of the Terfenol-D alloys by perfecting the preparation process or alloying. Mithun Palit et al. [8] studied the microstructural features and magnetic properties of alloy $\text{Tb}_{0.3}\text{Dy}_{0.7}\text{Fe}_{1.95-x}\text{Nb}_x$ ($x = 0–0.075$). The results showed that Nb addition results in the formation of NbFe_2 , inhibits the precipitation of the harmful phase REFe_3 phase, and

enhances the magnetostriptive properties of the alloy. Li Xiaocheng et al. [9] researched the microstructure and magnetostriiction of $\text{Tb}_{0.3}\text{Dy}_{0.7}\text{Fe}_{1.95-x}\text{Nb}_x$ ($x = 0, 0.03, 0.06, 0.09$) Alloys. Results demonstrated that the matrix phase still keeps cubic Laves phase with MgCu_2 (C15-type) structure with the addition of Nb. And the formation of the NbFe_2 phase suppresses the formation of the deleterious REFe_3 phase, thus making the magnetostriiction a little improvement as compared to the $\text{Tb}_{0.3}\text{Dy}_{0.7}\text{Fe}_{1.95}$ alloy. As described above, previous studies have shown that the addition of Nb has a beneficial effect on the magnetic properties of TbDyFe alloys. However, little attention has been paid to the mechanical properties of the alloy, which is a critical restriction factor for its large-scale applications. Further investigation and improvement are needed for both the magnetic and the mechanical properties of the alloys with the addition of Nb. In this paper, both the magnetic and the mechanical properties of the alloys with the addition of Nb were studied comprehensively.

2. Experiment

The samples $(\text{Tb}_{0.3}\text{Dy}_{0.7})_x\text{Fe}_{2x}\text{Nb}_y$ ($y = 0, 0.01, 0.04, 0.07, 0.1$; $3x + y = 1$) were melted four times in an arc melting furnace under high purity argon atmosphere with materials of the following purities: Tb, Dy (99.99 wt%), Fe, Nb (99.95 wt%). Phase constitution of the alloy were identified by X-ray diffraction (XRD) on a D8-Advance diffraction meter (Cu $K\alpha$ radiation, $\lambda = 0.154 \text{ nm}$) at a

* Corresponding author at: School of Materials Science and Engineering, Tsinghua University, Beijing 100084, PR China.

E-mail address: yuanliu@tsinghua.edu.cn (Y. Liu).

scanning rate of 6 min^{-1} . The XRD profiles were fitted by JADE 5.0 XRD analytical software (Materials Data, Inc., Livermore, CA) to eliminate the $K\alpha_2$ radiation. The microstructure and chemical composition as well as fracture morphology were characterized by means of a field emission scanning electron microscopy (FESEM) (Zeiss MERLIN-VP-COMPACT) equipped with an energy dispersive X-ray (EDX) (Oxford INCA) analyzer. The macro Vickers hardness of the alloy was measured by HVS-10 Vickers durometer with a load of 500 g for 30 s. And the fracture toughness K_{IC} of the material was calculated by the Vickers hardness indentation method. Micro Vickers hardness measurements were conducted by FM-800 microhardness tester under a load of 25gf applied for 20 s. Room temperature compression test was conducted on Gleeble-3500D thermal-mechanical simulator under an initial strain rate of 0.0001 s^{-1} . Cylindrical specimens for compression testing were 4 mm in diameter and 6 mm in height. The static

measurement of magnetostriction was tested by standard strain gauge with the sample size of $4 \times 4 \times 6 \text{ cm}^3$.

3. Results and discussion

3.1. Microstructure

Fig. 1 shows the X-ray diffraction patterns of alloy (a) $\text{Tb}_{0.3}\text{Dy}_{0.7}\text{Fe}_2$; (b) $(\text{Tb}_{0.3}\text{Dy}_{0.7})_{0.33}\text{Fe}_{0.66}\text{Nb}_{0.01}$; (c) $(\text{Tb}_{0.3}\text{Dy}_{0.7})_{0.32}\text{Fe}_{0.64}\text{Nb}_{0.04}$; (d) $(\text{Tb}_{0.3}\text{Dy}_{0.7})_{0.31}\text{Fe}_{0.62}\text{Nb}_{0.07}$; (e) $(\text{Tb}_{0.3}\text{Dy}_{0.7})_{0.3}\text{Fe}_{0.6}\text{Nb}_{0.1}$. The indices (hkl) of the Laves phase are also indexed in Fig. 1. It can be seen that all the alloys are essentially the REFe_2 phase with (2 2 0) and (3 1 1) crystal orientation. However, the intensity for (2 2 0) and (3 1 1) peaks of the REFe_2 phase decrease with the increase of the Nb content. It intuitively indicates that the formation of NbFe_2 phase causes a decrease in amount of REFe_2 phase, but an increase in rare earth-rich phase in the alloys.

Fig. 2 exhibits the BSEM images of the alloy (a) $\text{Tb}_{0.3}\text{Dy}_{0.7}\text{Fe}_2$; (b) $(\text{Tb}_{0.3}\text{Dy}_{0.7})_{0.33}\text{Fe}_{0.66}\text{Nb}_{0.01}$; (c) $(\text{Tb}_{0.3}\text{Dy}_{0.7})_{0.32}\text{Fe}_{0.64}\text{Nb}_{0.04}$; (d) $(\text{Tb}_{0.3}\text{Dy}_{0.7})_{0.31}\text{Fe}_{0.62}\text{Nb}_{0.07}$; (e) $(\text{Tb}_{0.3}\text{Dy}_{0.7})_{0.3}\text{Fe}_{0.6}\text{Nb}_{0.1}$. The phase compositions (EDS) of alloy (a–e) (at.%) are given in Table 1. The alloys are composed of three phases, including gray REFe_2 phase, white RE-rich phase, and dark NbFe_2 phase, as clearly demonstrated in Fig. 2. The phase compositions compiled in Table 1 indicates negligible solubility of Nb in the $(\text{Tb,Dy})\text{Fe}_2$ and (Tb,Dy) -rich phases. And the atom ratio of Nb: Fe is close to 1: 2 in the NbFe_2 compounds, so that the presence of the NbFe_2 precipitation phase is truly confirmed. Both the content of dark NbFe_2 phases and white rare earth-rich phases are increased gradually from the alloy (a) to alloy (e) with the increasing of Nb, as shown in Fig. 2. In addition, due to the addition of Nb element, the precipitation of harmful phase REFe_3 phase is inhibited in the alloy, which is consistent with the previous studies [8,9].

3.2. Magnetostriction

Fig. 3 demonstrates the intrinsic magnetostrictive curve of the alloy (a) $\text{Tb}_{0.3}\text{Dy}_{0.7}\text{Fe}_2$; (b) $(\text{Tb}_{0.3}\text{Dy}_{0.7})_{0.33}\text{Fe}_{0.66}\text{Nb}_{0.01}$; (c) $(\text{Tb}_{0.3}\text{Dy}_{0.7})_{0.32}\text{Fe}_{0.64}\text{Nb}_{0.04}$; (d) $(\text{Tb}_{0.3}\text{Dy}_{0.7})_{0.31}\text{Fe}_{0.62}\text{Nb}_{0.07}$; (e) $(\text{Tb}_{0.3}\text{Dy}_{0.7})_{0.3}\text{Fe}_{0.6}\text{Nb}_{0.1}$.

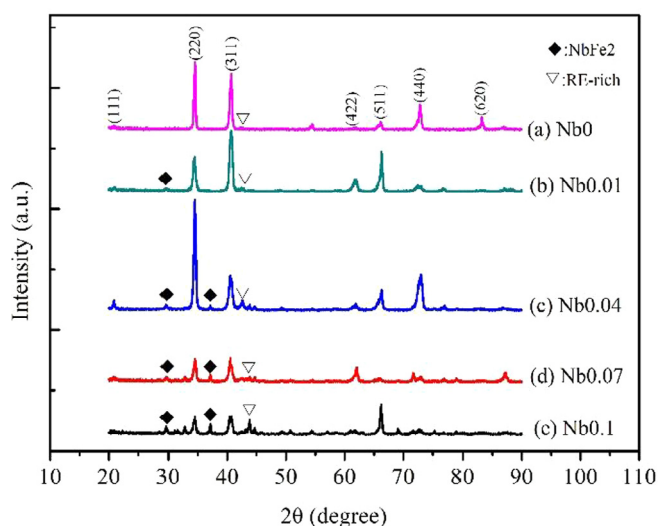


Fig. 1. X-ray diffraction patterns of alloy (a) $\text{Tb}_{0.3}\text{Dy}_{0.7}\text{Fe}_2$; (b) $(\text{Tb}_{0.3}\text{Dy}_{0.7})_{0.33}\text{Fe}_{0.66}\text{Nb}_{0.01}$; (c) $(\text{Tb}_{0.3}\text{Dy}_{0.7})_{0.32}\text{Fe}_{0.64}\text{Nb}_{0.04}$; (d) $(\text{Tb}_{0.3}\text{Dy}_{0.7})_{0.31}\text{Fe}_{0.62}\text{Nb}_{0.07}$; (e) $(\text{Tb}_{0.3}\text{Dy}_{0.7})_{0.3}\text{Fe}_{0.6}\text{Nb}_{0.1}$.

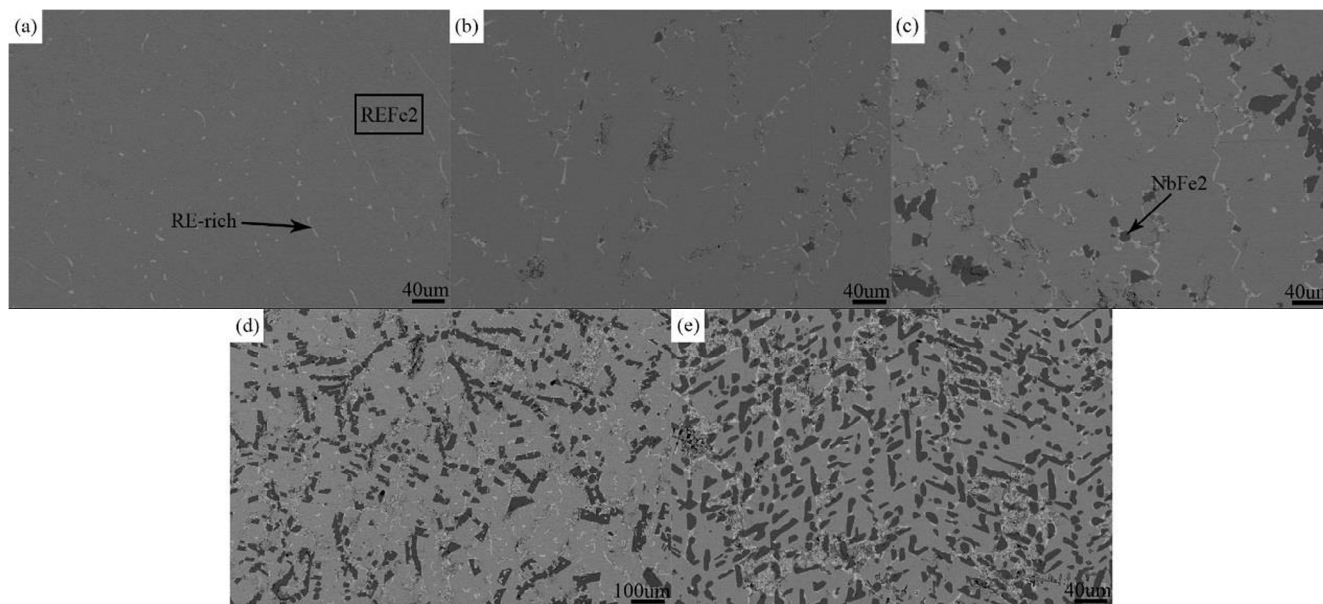


Fig. 2. BSEM images of the alloy (a) $\text{Tb}_{0.3}\text{Dy}_{0.7}\text{Fe}_2$; (b) $(\text{Tb}_{0.3}\text{Dy}_{0.7})_{0.33}\text{Fe}_{0.66}\text{Nb}_{0.01}$; (c) $(\text{Tb}_{0.3}\text{Dy}_{0.7})_{0.32}\text{Fe}_{0.64}\text{Nb}_{0.04}$; (d) $(\text{Tb}_{0.3}\text{Dy}_{0.7})_{0.31}\text{Fe}_{0.62}\text{Nb}_{0.07}$; (e) $(\text{Tb}_{0.3}\text{Dy}_{0.7})_{0.3}\text{Fe}_{0.6}\text{Nb}_{0.1}$.

Download English Version:

<https://daneshyari.com/en/article/8153955>

Download Persian Version:

<https://daneshyari.com/article/8153955>

[Daneshyari.com](https://daneshyari.com)